Restoring Motor Functions in Paralyzed Limbs through Intraspinal Multielectrode Microstimulation Using Fuzzy Logic Control and Lag Compensator

Amir Roshani[1], Abbas Erfanian [1*]

1. Iran Neural Technology Centre, Department of Biomedical Engineering, Iran University of Science and Technology (IUST), Tehran, Iran.

Article info:

Received: 23 Feb 2013

First Revision: 04 March 2013

Accepted: 05 May 2013

Key Words:

Functional Electrical Stimulation,
Intraspinal Microstimulation,
Fuzzy Logic Control,
Motor Function.

ABSTRACT

In this paper, a control strategy is proposed for control of ankle movement on animals using intraspinal microstimulation (ISMS). The proposed method is based on fuzzy logic control. Fuzzy logic control is a methodology of intelligent control that mimics human decision-making process. This type of control method can be very useful for the complex uncertain systems that their mathematical model is unknown. To increase the stability and speed of the system's response and reduce the steady-state error, we combine the FLC with a lead (lag) compensator. The experiments are conducted on five rats. Microelectrodes are implanted into the spinal cord to provide selective stimulation of plantarflexor and dorsiflexor. The results show that motor functions can be restored using ISMS. Despite the complexity of the spinal neuronal networks and simplicity of the proposed control strategy, our results show that the proposed strategy can provide acceptable tracking control with fast convergence.

1. Introduction

Functional electrical stimulation (FES) is a potentially useful technique to restore motor functions in individuals with spinal cord injury, head injury, stroke, and multiple sclerosis (Agarwal et al., 2003; Hardin et al., 2007). Currently, FES systems utilize peripheral nerve stimulation or direct muscle stimulation to restore motor functions. Though some advances have been achieved by traditional FES systems, there are still unsolved problems. The challenge of peripheral nerve stimulation or direct muscle stimulation is the physiological recruitment order of motor units (Tai & Jiang, 1994) and the muscle fatigue. Larger motor units are activated physiologically after smaller ones have been recruited according to the "size principle" (Fang & Mortimer, 1991; Karu, Durfee, & Durfee, 1995). However, in conventional FES, larger motor units are excited before smaller ones. This type of "reverse recruitment" order and synchronized activation result in poor force gradation and rapid muscle fatigue for electrically activated muscles (Fang & Mortimer, 1991; Karu et al., 1995).

To overcome the difficulties of the traditional FES systems (nerve or direct muscle stimulation), intraspinal microstimulation (ISMS) has been recently proposed as a means to activate the paralyzed skeletal muscle through electrical stimulation of the lumbo-sacral portion of the spinal cord (Pikov, 2008). The spinal cord contains neuronal circuitry called motor neuron pools. All of the motor neurons in a motor neuron pool innervate a single muscle, and all motor neurons that innervate a particular muscle are contained in the same motor neuron pool. Each individual muscle fiber in a muscle is innervated by one, and only one, motor neuron. However, a single

**** Corresponding Author:***
Abbas Erfanian, PhD.
Iran Neural Technology Centre, Department of Biomedical Engineering, Iran University of Science and Technology (IUST), Tehran, Iran.
Tel: +98-21-77240465/ Fax: +98-21-77240253
E-mail: erfanian@iust.ac.ir

motor neuron can innervate many muscle fibers. Therefore, different groups of muscles could potentially be selectively activated by implanting microelectrodes into different motor-pools.

It has been demonstrated that ISMS has several advantages over peripheral nerve or direct muscle stimulation (Tai, Booth, Robinson, de Groat & Roppolo, 1999; Tai, Booth, Robinson, de Groat & Roppolo, 2000; Mushahwar & Horch, 2000). It was shown that graded muscle contraction in individual muscle or muscle groups could be generated by electrically stimulating motor neurons in the lumbo-sacral of spinal cord (Bamford, Putman, & Mushahwar, 2005). The gradual force recruitment characteristics of ISMS have been attributed to its ability to activate motor neurons in a near normal physiological order based on their size (Fang & Mortimer, 1991). It was demonstrated that intramuscular stimulation is characterized by rapid muscle fatigue and that ISMS is able to elicit prolonged and stable force generation (Lau, Guevremont, & Mushahwar, 2007).

Although ISMS is expected to have several advantages over peripheral nerve or direct muscle stimulation, several challenging problems remain to be solved. An important issue is the selective stimulation of the hind limb muscles. Mushahwar and Horch (2000) demonstrated that the selective activation of muscle groups can be achieved through ISMS. They showed that the selective activation of quadriceps, tibialis anterior or triceps surae/plantaris muscles occurs when the target muscle's motor pool is directly stimulated. However, increasing the stimulation intensity to increase the force level and the ranges of motion causes the spread of current to adjacent motor pools and the activation of the other motor pools.

To solve this problem, we have already demonstrated that the selective activation of the muscle can be enhanced by delivering the stimulation signal through the electrodes at multiple locations within a given motor activation pool (Roshani & Erfanian, 2012). Mushahwar and Horch (1997) showed that fatigue is essentially eliminated by interleaved stimulation when the stimuli are delivered through two separate electrodes simultaneously in an interleaved manner. Moreover, they demonstrated that the values of mean and standard deviation of force increase during simultaneous stimulation through two electrodes compared to the sum of the forces generated by stimulation through each electrode alone.

Tai et al. (2000) used three different electrode combinations (single electrode only, electrode pairs and three electrodes) for evaluating the effects of multielectrode ISMS. They showed that the isometric torque evoked by ISMS with a three electrode combination could be enhanced or suppressed when compared with that evoked by single or paired electrode stimulation. Lemay, Galagan, Hogan, and Bizzi (2001) evaluated the responses produced by coactivation of two spinal sites in frog. They found that for multielectrode stimulation, the forces under coactivation were the scaled vectorial summation of the individual responses.

All these studies demonstrated the several benefits of the ISMS through a distributed set of electrodes implanted in a given motor activation pool including finer control of force generation, selective activation, and fatigue resistance. Another important challenge to the restoration of paralyzed motor function through the use of ISMS is the control strategy for generation of appropriate electrical stimulation patterns. In previous work (Asadi & Erfanian, 2012), we developed a robust control strategy for movement control via ISMS using a single electrode implanted in each motor pool within the spinal cord. In the current study, we develop a control strategy for control of ankle movement using ISMS via two microelectrodes implanted in motor pool of each muscle. A major problem to control of such systems is the highly nonlinear and time-varying properties that are exposed to strong influence of internal and external disturbances. Moreover, developing an accurate model of such systems is totally impractical. One simple approach to deal with such systems is fuzzy logic control (FLC). Fuzzy control provides a formal methodology for representing, manipulating, and implementing a human's heuristic knowledge about how to control a system. In this paper, we use FLC for control of movement using ISMS.

2. Methods

2.1. Controller Design

2.1.1. Structure of Controller

The configuration of the proposed control strategy is schematically depicted in Fig. 1. For each neuro-muscle-joint complex an independent controller is designed. Each controller has two outputs (i.e., stimulation signal) which are delivered to the spinal cord via two microelectrodes implanted in the motor pool of the muscle. The objective of the controllers is to generate stimulation signals to force the joint angle to track a desired trajectory in the presence of system uncertainties, time-delay, and disturbances.

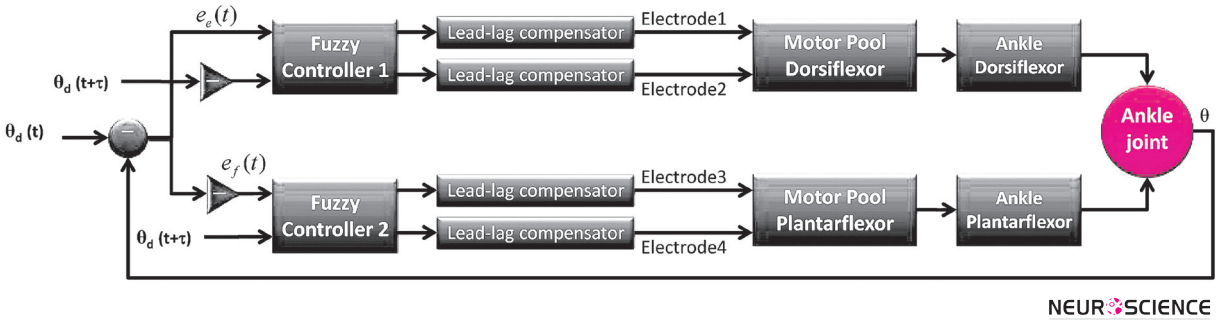

Figure 1. Block diagram of the proposed fuzzy logic control for control of the ankle movement using multielectrode intraspinal microstimulation (ISMS).

2.1.2. Fuzzy Logic Controller

The fuzzy controller has four main components (Fig. 2): fuzzy rules, fuzzification, fuzzy implication, and defuzzification (Kovacic & Bogdan, 2006).The fuzzification interface simply modifies the inputs so that they can be interpreted and compared to the rules in the rule-base. The conversion of a numerical value of x into a corresponding linguistic value by associating a membership function is called fuzzification. In the proposed FLC, inputs are the normalized error signal and the future value of the normalized desired trajectory. The fuzzy rule base is the central component of a fuzzy controller and it holds the knowledge in the form of a set of rules. The rule base includes a set of "if…then…" rules. Each rule describes a relationship between the input fuzzy sets and the output fuzzy sets. The inference engine evaluates which control rules are relevant at the current time and then decides what the input to the plant should be. In this paper, we use mamdani implication (Kovacic & Bogdan, 2006) to determine the influence produced by the antecedent part of the fuzzy rule on the consequent part of the rule. The defuzzification interface converts the conclusions reached by the inference mechanism into the inputs to the plant. In the proposed FLC, fuzzy sets consist of negative big (NB), negative small (NS), zero (Z), positive small (PS), positive medium (PM), and positive big (PB).

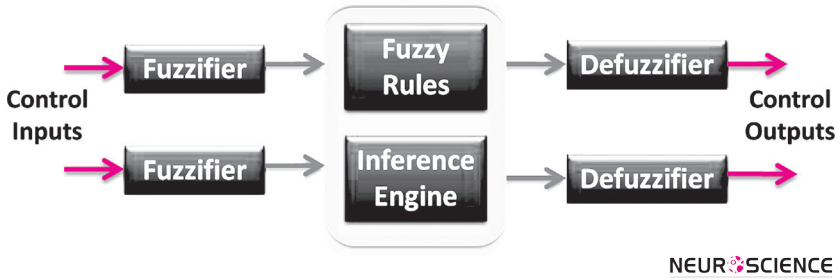

Figure 2. Structure of the fuzzy logic control (FLC).

Using the pre-defined fuzzy rule base (Table I), mamdani implication, singleton and Gaussian membership functions, sum–min aggregation, and the center of area (COA) defuzzification, the output of FLC can be defined as

$$u_{FLC}(x_k, y_k) = \frac{\sum_i u_i . \mu_u(x_k, y_k, u_i)}{\sum_i \mu_u(x_k, y_k, u_i)} \quad (1)$$

where

$$\mu_u(x_k, y_k, u) = \sum \min_{i=1}^{r} \left[\mu_{R_{pq}}(x_k, y_k), \mu_{P_m}(u) \right] \quad (2)$$

where $u_{FLC}(x_k, y_k)$ represents the crisp value of the fuzzy controller output, u_i is a discrete element of an output fuzzy set and $\mu_u(x_k, y_k, u_i)$ is its membership function, R_{pq} and P_m are antecedent and consequent parts of the fuzzy rule, respectively, denotes a number of fuzzy rules activated by x_k and y_k and $\mu_u(x_k, y_k, u_i)$.

2.1.3. Lead (lag) Compensator

The purpose of lag compensator is to, improve the transient response characteristics by increasing the phase margin of the system, and reduce the steady-state error

by increasing only the low-frequency gain. The lead compensator increases the bandwidth by increasing the gain crossover frequency to realize a faster transient response. The lead or lag compensator is described by a transfer function

$$G_f(s) = K_f \frac{T_f s + 1}{T_M s + 1} \quad (3)$$

where K_f is the gain coefficient, T_f is the lead-time constant and T_M is the desired time constant.

If $T_f \leq T_M$ transfer function (3) will be a lead compensator and if $T_f \leq T_M$ it will be a lag compensator. Depending on desired response any combination of lead and lag compensator can be used (Kovacic & Bogdan, 2006).

2.2. Experimental Setup

2.2.1. Animal Preparation

Five male adult Wistar rats (350-400 g) were used in this study. Five sessions of experiment were performed (each session on a rat). The rats were anesthetized with intraperitoneal injection of urethane (1.65 g/kg). Then a partial laminectomy was performed to expose the T12-L2 segments and the dura mater over these laminas was opened longitudinally. The rats were placed in a stereotaxic frame (SR-6R, Narishige Group Product) which allowed hindlimbs to move freely (Fig. 3). All surgical procedures and experimental protocols were approved by the local ethics committee.

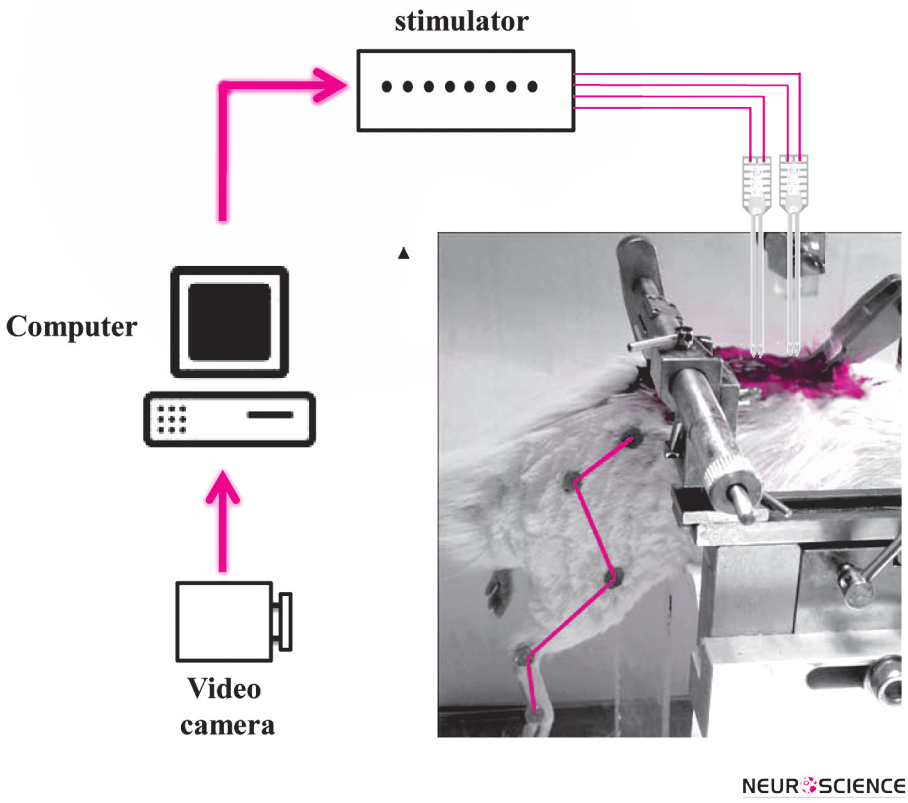

Figure 3. Schematic of the experimental setup for closed-loop control of the knee movement using ISMS.

2.2.2. Data Acquisition and Stimulation Electrode

To measure the joint angles, colored markers were attached to each link. A webcam was focused to capture the location of the markers during limb movements elicited by ISMS. We used NI Vision development module in LabVIEW to estimate the joint angles.

An eight-channel computer based stimulator (STG4008 -1.6mA Multi Channel Systems MCS GmbH) was used to stimulate the spinal cord. The stimulator can generate charge balanced, biphasic current pulses. The amplitude, pulse width, and frequency of the stimulation signal can be varied online using custom software package written in LabVIEW. Stimulus pulses were delivered through a

custom-made multi-electrode array implanted in the ventral horn of the L1 spinal segment. The multi-electrode array was made of tungsten electrodes (127 µm in diameter, A-M Systems, WA) with fixed inter-electrode spacing of 300 µm. The stimulating electrode was mounted in a Narishige micromanipulator which controlled its three-dimensional position in the lumbo-sacral portion of the spinal cord.

2.2.3. Experimental Procedure

Multielectrode array was positioned at the locations within the ventral horn where selective stimulation of the dorsiflexor (plantar flexor) muscle could be obtained by each electrode. To determine the best electrode position for selective muscle stimulation, the electrode array was vertically advanced through the spinal cord in 50 µm steps, dorsoventrally, and then, the electrode was withdrawn and moved 100 µm mediolaterally and/or rostrocaudally to an adjacent location where the testing was repeated. At each stop along the electrode track, biphasic pulses with 80-µs duration, 60-µA amplitude, and 50-Hz frequency were delivered to the spinal cord through the microelectrode to identify the effective positions for selective dorsiflexion (plantar flexion). The positions that produced the highest movement range on the ankle joint and the least effect on the other joints were selected. Two electrodes were implanted in each motor pool of the muscle with 300-µm spacing.

In the current study, pulse amplitude (PA) modulation at a constant frequency (50 Hz) and constant pulse width (PW) was used to stimulate the spinal cord. The proposed control strategy was implemented with LabVIEW. The period for control updates was 20 ms. The interleave time between two electrodes implanted into a motor pool was set to zero (i.e., no stimulus interleave time).

3. Results

In this section, the performance of the proposed control strategy is evaluated. For this purpose, the controller is first applied on a mathematical model of musculoskeletal system. Then, the results of experiments on rats are presented.

We use the root-mean-square (RMS) error and normalized RMS (NRMS) as the performance indices to measure the tracking accuracy as

$$\mathrm{RMS} = \sqrt{\frac{1}{T}\sum_{t=1}^{T}\left(\theta(t)-\theta_d(t)\right)^2} \qquad (4)$$

$$\mathrm{NRMS}(\%) = \frac{1}{\left(\theta_d^{\max}-\theta_d^{\min}\right)}\sqrt{\frac{1}{T}\sum_{t=1}^{T}\left(\theta(t)-\theta_d(t)\right)^2}\times 100 \qquad (5)$$

where θ and θ_d are the measured and desired joint angle, respectively.

3.1. Simulation Studies

A model of musculoskeletal system which was presented in (Abbas & Chizeck, 1995) is used here to simulate ankle joint movement. The model consists of two pairs of agonist-antagonist muscles (i.e., two flexors and two extensors) acting around the joint. The model of electrically stimulated muscle that is used in this study includes a 50-ms time-delay, nonlinear recruitment, linear dynamics and multiplicative nonlinear torque-angle and torque-velocity scaling factors. To consider the processing time, stimulator delay, and video frame capture time, a 100 ms delay is also considered. The virtual joint consists of a single skeletal segment in a swing pendulum configuration with one degree-of-freedom. The skeletal segment is acted upon by an agonist–antagonist pair of electrically stimulated muscles. The set of parameters for muscle and skeletal model are taken from (Abbas & Chizeck, 1995). The parameters of the compensator were selected as follows:

$$K_f = 1, \quad T_f == 0.25, \quad T_M = 0.1.$$

The value of was set to 150 ms (i.e., the total system delay). The future value of desired trajectory was normalized to values between -1 and 1. The error signals used for extensor and flexor controllers were calculated by

$$\begin{bmatrix} e_e \\ e_f \end{bmatrix} = \begin{bmatrix} +1 \\ -1 \end{bmatrix}\left[\theta - \theta_d\right]$$

where e_e and e_f are the error signals for controllers of the flexor and extensor, respectively; θ is the measured joint angle, and θ_d is the reference trajectory.

Fig. 4(a) shows the result of the FLC of the simulated ankle joint angle using only error signal ($e(t)$) as the input of the controller and without using compensator. The result shows that the tracking error is 8.3° (20.8%). The results of the control of simulated ankle joint using FLC with both $e(t)$ and $\theta(t+\tau)$ as the inputs of the controller is shown in Fig. 4(b). The RMS (NRMS) tracking error is 4.4° (11.0%). The results of tracking control using the proposed FLC (Fig. 1) is shown in Fig. 4(c) [RMS error

2.0° (5.0%)]. The results show that the tracking performance is improved by the proposed FLC. An interesting observation is the fast convergence of the controller. The generated joint angle converges to its desired trajectory in less than 0.5 s. Figure 4 shows that there is a low level of co-activation at the low activation levels. The level of agonist–antagonist co-activation tends to decrease as the muscle activation increases.

Effects of External Disturbance: To evaluate the ability of proposed control strategy to external disturbance rejection, a 20 Nm constant torque (which is about 20% of maximum generated torque during disturbance-free trial) was added to the torque generated by the muscles. Fig. 5 shows the result of tracking performance during applying the disturbance. It is observed that an acceptable disturbance rejection is achieved using the proposed

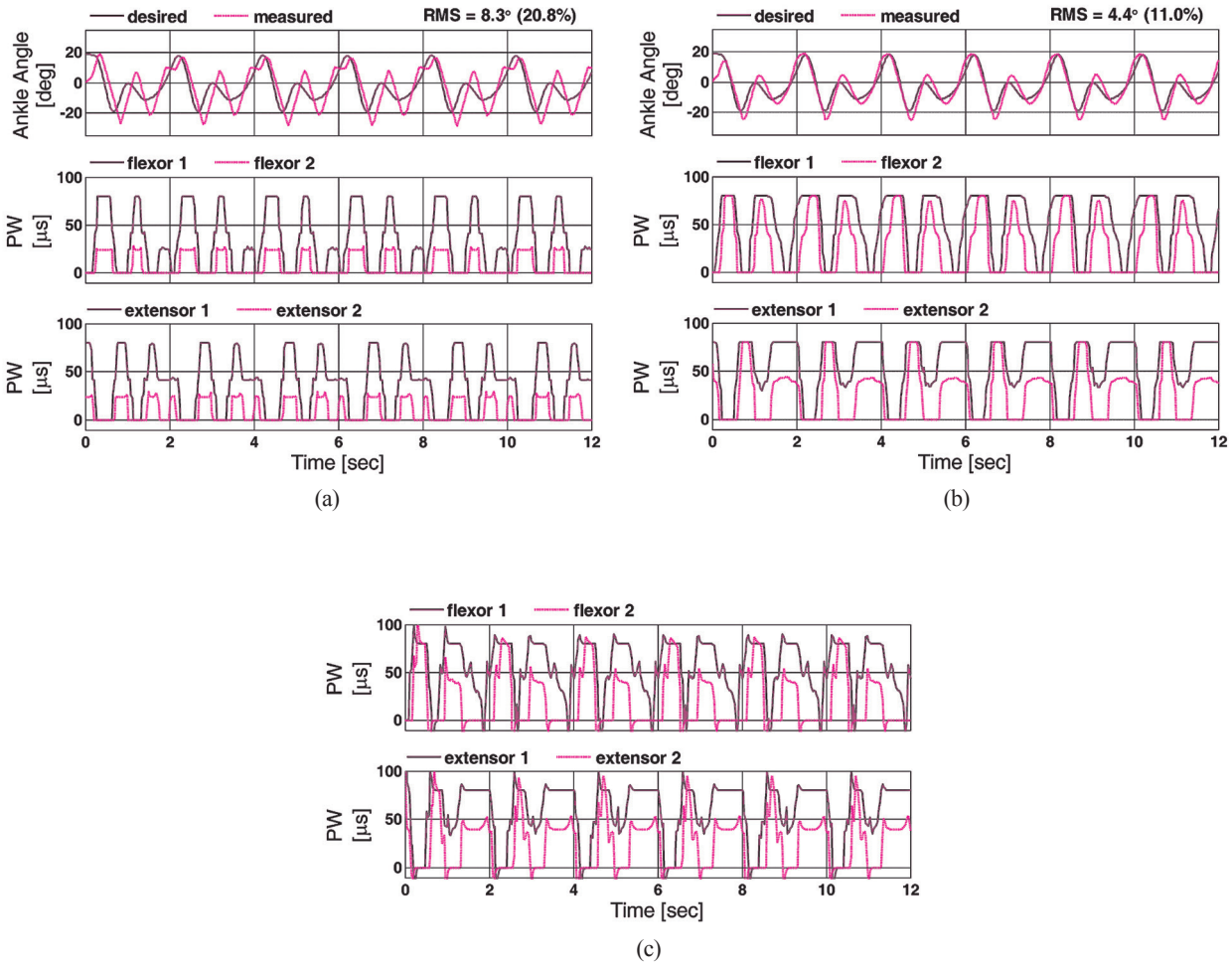

NEUROSCIENCE

Figure 4. Simulation results of joint movement control using fuzzy logic control. (a) Using FLC with only error signal as the input (b) Using FLC with both error signal and feature value of the desired trajectory as the inputs of the controller (c) Using FLC (both error signal and feature value of the desired trajectory as the inputs of the controller) combined with the lead-lag compensator.

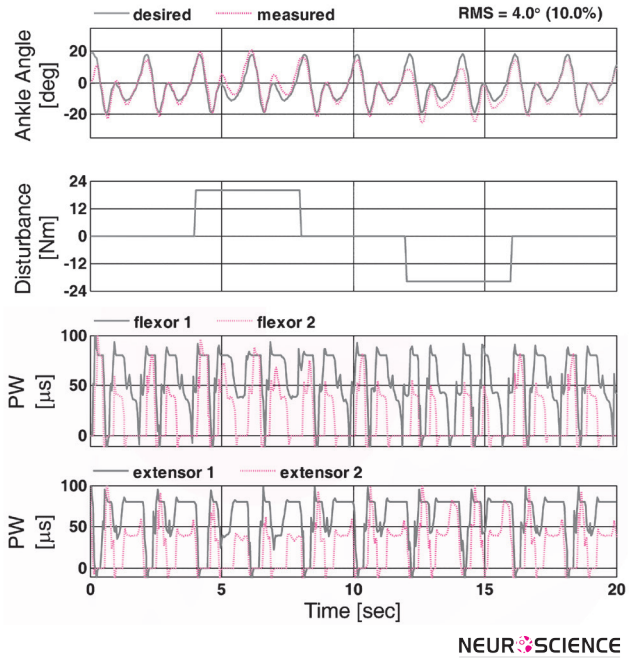

Figure 5. Simulation results of an external disturbance rejection using the proposed FLC. A constant torque in amount of 20 Nm (which is approximately 20% of the peak generated torque during the disturbance-free trial) was added to and subtracted from the net torque generated by the muscles for a duration of 4s. The bottom plot shows the control outputs (i.e., stimulation signals).

FLC. The tracking error obtained during disturbance is 4.0° (10.0%). Positive torque causes joint extension and negative torque causes joint flexion. It is observed that during positive disturbance, the flexor stimulation signals were increased and the extensor stimulation signals were decreased to compensate for the effects of disturbance.

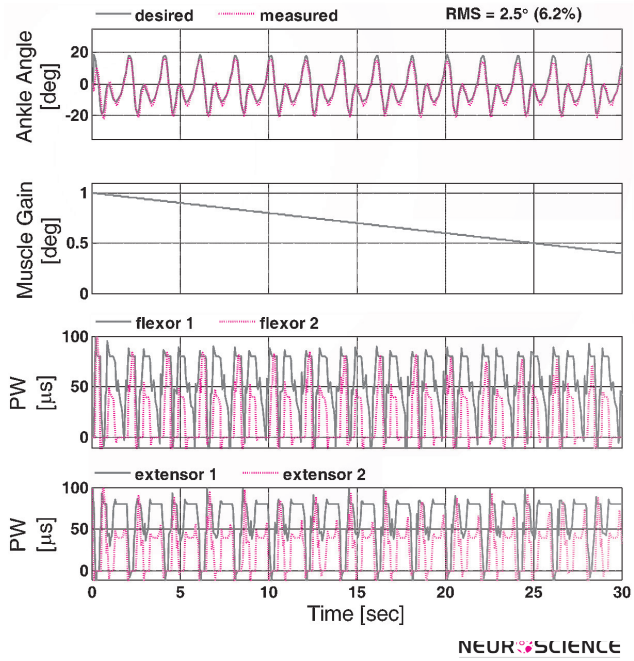

Figure 6. Simulation result of fatigue compensation obtained by the proposed FLC. The effects of muscle fatigue were simulated by exponentially decreasing the muscle input gains during the course of the simulation.

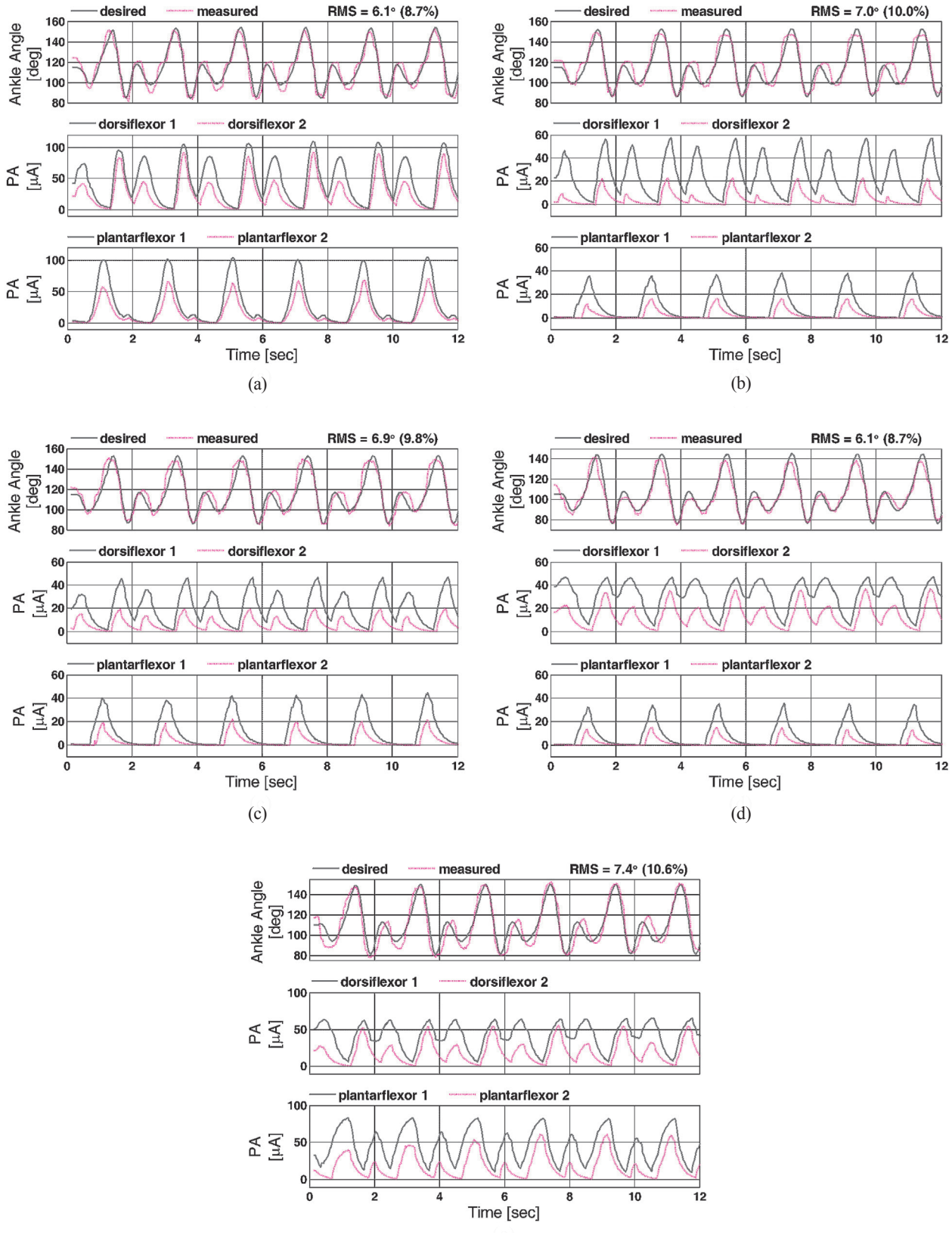

Figure 7. Typical results of controlling plantarflexion and dorsiflexion using the proposed FLC on five rats. (a) Rat 1 (b) Rat 2 (c) Rat 3 (c) Rat 4 (d) Rat 5. The bottom plots show the stimulation signals delivered through four electrodes (dorsiflexor 1, dorsiflexor 2, plantarflexor 1, plantarflexor 2).

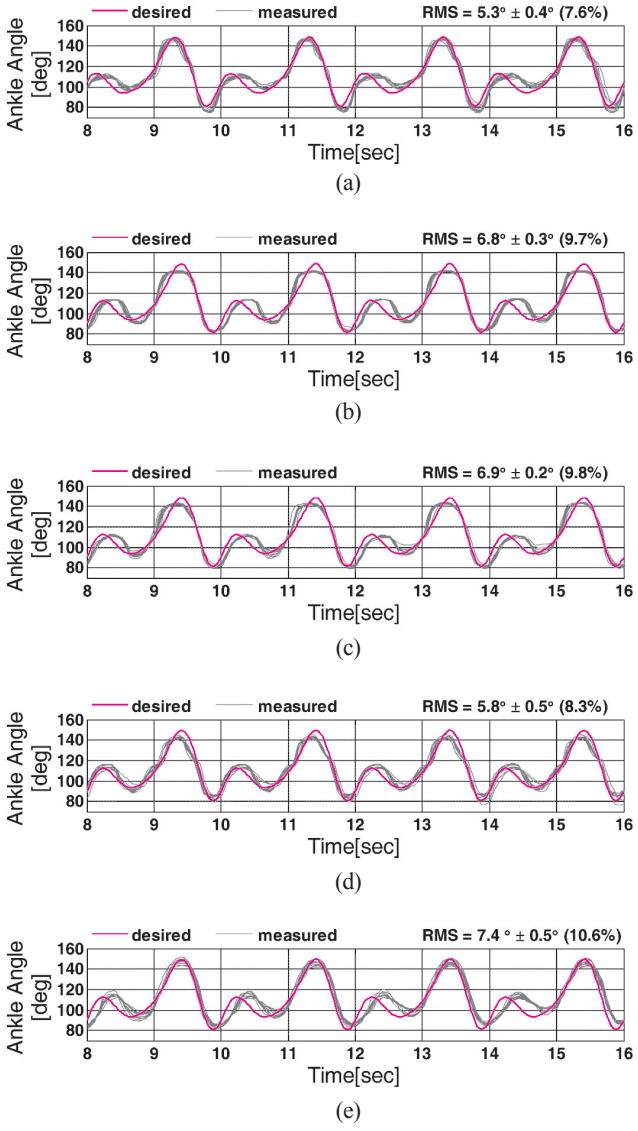

Figure 8. Results of the ankle movement control using the proposed FLC during ten trials of experiment on five rats.

Table 1. Fuzzy rule base

$\Theta(t+\tau)$ \ e		BN	SN	Z	SP	BP
BN	Out1	Z	Z	Z	Z	Z
	Out2	Z	Z	Z	Z	Z
SN	Out1	M	Z	Z	Z	Z
	Out2	Z	Z	Z	Z	Z
Z	Out1	B	M	Z	Z	Z
	Out2	Z	Z	Z	Z	Z
SP	Out1	B	B	S	Z	Z
	Out2	M	Z	Z	Z	Z
BP	Out1	B	B	B	M	Z
	Out2	B	M	Z	Z	Z

Table 2. Average Root-Mean-Square tracking error obtained during ten experimental trials using proposed control strategy for different rats.

Trial	Rat 1	Rat 2	Rat 3	Rat 4	Rat 5
1	6.1°	7.0°	6.9°	6.1°	7.4°
2	5.5°	6.8°	6.8°	6.9°	8.1°
3	5.6°	6.7°	7.0°	5.6°	7.7°
4	5.3°	6.8°	7.1°	5.4°	7.1°
5	5.2°	6.8°	6.7°	5.2°	7.2°
6	5.3°	6.1°	6.8°	5.6°	8.5°
7	5.1°	6.4°	7.0°	5.8°	7.1°
8	5.3°	7.0°	6.8°	5.8°	6.9°
9	4.7°	7.2°	6.5°	5.5°	7.0°
10	5.1°	6.8°	7.0°	5.8°	7.2°
Mean±STD	5.3°±0.4°	6.8°±0.3°	6.9°±0.2°	5.8°±0.5°	7.4°±0.5°
NRMS	7.6%	9.7%	9.8%	8.3%	10.6%

NEUROSCIENCE

Effects of Muscle Fatigue: In FES applications, muscle fatigue can cause degradation of system performance. To evaluate the ability of the controller to account for muscle fatigue, the effects of muscle fatigue were simulated by a linear decrease in the agonist's (antagonist's) input gain to 40% of its original value over 30 s. Fig. 6 shows the result of fatigue compensation using the proposed controller [RMS error 2.5° (6.2%)]. It is observed that, during prolonged stimulation, the levels of the stimulation signals were increased to compensate the effects of muscle fatigue.

3.2. Experimental Evaluation

In this section, the performance of employing the proposed control strategy on animals is presented. The experiments were conducted on five rats. The parameters of the compensator (i.e. and) were chosen heuristically to achieve the best controller performance during experimental studies as follows:

k_f=1, T_f== 0.05, T_M= 0.2.

To implement the proposed fuzzy logic controller, it is necessary to estimate the time-delay (i.e.,). To estimate the time-delay, a 1.5-s long sequence of pulses with constant width and constant amplitude was delivered to the motor pools and time delay was estimated experimentally. The results showed that there was approximately a 200 ms time-delay in response.

Examples of the ankle joint angle trajectories obtained with the proposed FLC during one experimental trial for five rats are shown in Fig. 7. The results show that a good tracking performance with fast convergence is achieved. The RMS errors obtained during the first trial of experiment are 6.1° (8.7%), 7.0° (10.0%), 6.9° (9.8%), 6.1° (8.7%), and 7.4° (10.6%) for rat1, rat2, rat3, rat4, and rat5, respectively. Almost the same results were obtained in all experimental trials on all rats. The control signals (i.e., stimulation signal) show that there is antagonist co-activation during ankle movement. At the low levels of activation, both muscles are engaged. The activity of antagonist (agonist) decreases as agonist (antagonist) ac-

tivity increases. At the peak angles, there is no overlap between the agonist and antagonist muscles.

Table 2 summarizes the tracking errors obtained during 10 experimental trials for each rat. The average of tracking error over 10 experimental trials is 5.3°±0.4° (7.5%), 6.8°±0.3° (9.7%), 6.9°±0.2° (9.8%), 5.8°±0.5° (8.3%), and 7.4°±0.5° (10.6%), for rat1, rat2, rat3, rat4, and rat5, respectively. Standard deviation of the tracking errors is less than 0.5° that indicates the repeatability of the control performance over the different experimental trails and different rats.

Fig. 8 shows joint angle trajectories obtained using the proposed FLC during ten trials of experiment on five rats. The results clearly indicate that the controller is robust during different experimental trials.

4. Discussion

In this paper, we proposed a control strategy for control of ankle movement using multielectrode ISMS. The controller is based on the combination of fuzzy logic control with a lead (lag) compensator. The results indicate that motor functions can be restored through ISMS. The average of tracking error over the five rats is 6.4°±0.8° (9.2%). One important issue in the design of control strategy is time-delay. There is a significant time-delay in neuromuscular system response with respect to stimulation signal. The existence of the time-delays may be the source of instability and may degrade the performance of the closed-loop system. In this paper, we designed the fuzzy rules based on the future value of the desired trajectory to compensate the effect of the time-delay. For this purpose, a constant time-delay was considered. Nevertheless, the time-delay in neuromuscular system is time-varying. The time-varying delay needs a deeper analysis since its presence may induce complex behaviors. Moreover, in this study, we employed the proposed control strategy for control of the ankle joint during short period of stimulation. Future work will focus on the extension of this strategy to cope with uncertain time-varying time-delay for multi-joint control and control of locomotion using ISMS.

In this work, two microelectrodes were implanted into motor pool of each muscle and the fuzzy rule base was designed such that the stimulus was delivered first through one electrode. If the tracking error is still high and the future value of the desired trajectory is big, then the second electrode will be recruited. During multielectrode ISMS, electrical stimulation induced by a microelectrode can be made sufficiently focal so that only a small group of motoneurons will be activated. Designing a control strategy to activate motor units in the same muscle by focally stimulating several small groups of motoneurons asynchronously within the same motor pool is a challenging problem in ISMS control.

In this work, the parameters of the compensator were chosen heuristically to achieve the best controller performance. Optimal estimation of the parameters and stability analysis of the closed-loop system remain the key issues in fuzzy logic control of spinal cord.

Acknowledgement

This work was supported by Iran Neural Technology Centre, Iran University of Science and Technology, Tehran, Iran.

References

Abbas, J. J., & Chizeck H. J. (1995). Neural network control of functional neuromuscular stimulation systems: computer simulation studies. IEEE Trans. Biomed. Eng. 42(11), 1117-27.

Agarwal, S., Triolo, R. J., Kobetic, R., Miller, M., Bieri, C., Kukke, S., Rohde, L., & Davis, J. J. (2003). Long-term perceptions of an implanted neuroprosthesis for exercise, standing and transfers after spinal cord injury. J Rehabil. Res. Dev, 40(3), 241-252.

Asadi, A.-R., & Erfanian A. (2012). Adaptive neuro-fuzzy sliding mode control of multi-joint movement using intraspinal microstimulation. IEEE Trans Neural Syst Rehabil Eng, 20(4), 499-509.

Bamford, J. A., Putman, C. T., & Mushahwar, V. K. (2005). Intraspinal microstimulation preferentially recruits fatigue-resistant muscle fibres and generates gradual force in rat. Journal of Physiol, 569(3), 873-884.

Fang, Z.-P. & Mortimer, J. T. (1991). A method to effect physiological recruitment order in electrically activated muscle. IEEE Trans. Biomed. Eng, vol. 38, 38(2), 175-179.

Hardin, E., Kobetic, R., Murray, L., Corado-Ahmed, M., Pinault, G., Sakai, J., Bailey, S. S., Ho, C., & Triolo, R. J. (2007). Walking after incomplete spinal cord injury using an implanted FES system: a case report. J. Rehabil. Res. Dev, 44(3), 333-346.

Karu, Z. Z., Durfee, W. K., & Barzilai, A. M. (1995) . Reducing muscle fatigue in FES applications by stimulating with N-let pulse trains. IEEE Trans. Biomed. Eng, 42(8), 809-817.

Kovacic, Z., & Bogdan, S. (2006). Fuzzy controller design : theory and applications. Boca Raton, FL : CRC /Taylor & Francis.

Lau, B., Guevremont, L., & Mushahwar, V. K. (2007). Strategies for generating prolonged functional standing using intramuscular stimulation or intraspinal microstimulation. IEEE Transactions on Neural Systems and Rehabilitation Engineering, 15(2), 273-285.

Lemay, M. A., Galagan, J. E., Hogan, N., & Bizzi, E. (2001). Modulation and vectorial summation of the spinalized frog's hindlimb end-point force produced by intraspinal electrical stimulation of the cord. IEEE Transactions on Neural Systems and Rehabilitation Engineering, 9(1), 12-23.

Mushahwar, V. K., & Horch, K. W. (1997). Proposed specifications for a lumbar spinal cord electrode array for control of lower extremities in paraplegia. IEEE Transactions on Rehabilitation Engineering, 5(1), 237-243.

Mushahwar, V. K., & Horch, K. W. (2000). Muscle recruitment through electrical stimulation of the lumbo-sacral spinal cord. IEEE Trans. Rehabil. Eng, 8(1), 22-29.

Mushahwar, V. K., & Horch, K. W. (2000). Selective activation of muscle groups in the feline hindlimb through electrical microstimulation of the ventral lumbo-sacral spinal cord. IEEE Trans. Rehabil. Eng, 8(1), 11-21.

Pikov, V. (2008). Clinical applications of intraspinal microstimulation. Proceedings of the IEEE, 96(7), 273-285.

Roshani, A., & Erfanian, A. (2012). Influences of multielectrode stimulation and stimulation parameters on selective activation of motor pools in intraspinal microstimulation. 17th Annual Conference of the International Functional Electrical Stimulation Society.

Tai, C., & Jiang, D. (1994). Selective stimulation of smaller fibers in a compound nerve trunk with single cathode by rectangular current pulses. IEEE Trans. Biomed. Eng, 41(3), 286-291.

Tai, C., Booth, A. M., Robinson, C. J., de Groat, W. C., & Roppolo, J. R. (1999). Isometric torque about the knee joint generated by microstimulation of the cat L6 spinal cord. IEEE Transactions on Rehabilitation Engineering, 7(1), 46-55.

Tai, C., Booth, A. M., Robinson, C. J., de Groat, W. C., & Roppolo, J. R. (2000). Multimicroelectrode stimulation within the cat L6 spinal cord: Influences of electrode combinations and stimulus interleave time on knee joint extension torque. IEEE Transactions on Rehabilitation Engineering, 8(1), 1-10.